Regenerative Therapy 4 (2016) 9–17

Contents lists available at ScienceDirect

Regenerative Therapy

journal homepage: http://www.elsevier.com/locate/reth

Original article

Electrophysiological properties of iPS cell-derived cardiomyocytes from a patient with long QT syndrome type 1 harboring the novel mutation M437V of KCNQ1

Tatsufumi Sogo [a], Kumi Morikawa [b], Yasutaka Kurata [c, *], Peili Li [a], Takafumi Ichinose [a], Shinsuke Yuasa [d], Daizou Nozaki [a], Junichiro Miake [e], Haruaki Ninomiya [f], Wataru Shimizu [g], Keiichi Fukuda [d], Kazuhiro Yamamoto [e], Yasuaki Shirayoshi [a], Ichiro Hisatome [a, b]

[a] Division of Regenerative Medicine and Therapeutics, Department of Genetic Medicine and Regenerative Therapeutics, Tottori University Graduate School of Medical Science, 86 Nishi-cho, Yonago 683-8503, Japan
[b] Center for Promoting Next-Generation Highly Advanced Medicine, Tottori University Hospital, 36-1 Nishi-cho, Yonago 683-8504, Japan
[c] Department of Physiology, Kanazawa Medical University, 1-1 Daigaku, Uchinada-machi, Ishikawa 920-0293, Japan
[d] Department of Cardiology, Keio University School of Medicine, 35 Shinano-machi Shinjuku-ku, Tokyo 160-8582, Japan
[e] Division of Cardiovascular Medicine, Endocrinology and Metabolism, Department of Molecular Medicine and Therapeutics, Tottori University Faculty of Medicine, 86-1 Nishi-cho, Yonago 683-8504, Japan
[f] Department of Biological Regulation, School of Health Science, Tottori University Faculty of Medicine, 36-1 Nishi-cho, Yonago 683-8503, Japan
[g] Department of Cardiology, Nippon Medical School, 1-1-5 Sendagi, Bunkyo-ku, Tokyo 113-8603, Japan

ARTICLE INFO

Article history:
Received 2 October 2015
Received in revised form
17 December 2015
Accepted 24 December 2015

Keywords:
KCNQ1
LQT1
iPS cell
C-terminus mutation
Early afterdepolarization

ABSTRACT

Introduction: Long QT syndrome type 1 (LQT1) is caused by mutations in KCNQ1 coding slowly-activating delayed-rectifier K^+ channels. We identified the novel missense mutation M437V of KCNQ1 in a LQT1 patient. Here, we employed iPS cell (iPSC)-derived cardiomyocytes to investigate electrophysiological properties of the mutant channel and LQT1 cardiomyocytes.

Methods: To generate iPSCs from the patient and a healthy subject, peripheral blood T cells were reprogrammed by Sendai virus vector encoding human OCT3/4, SOX2, KLF4, and c-MYC. Cardiomyocytes were prepared from iPSCs and human embryonic stem cells using a cytokine-based two-step differentiation method and were subjected to patch clamp experiments.

Results: LQT1 iPSC-derived cardiomyocytes exhibited prolongation of action potential duration (APD), which was due to a reduction of the KCNQ1-mediated current I_{Ks}; Na^+, Ca^{2+} and other K^+ channel currents were comparable. When expressed in HEK293 and COS7 cells, the mutant KCNQ1 was normally expressed in the plasma membrane but generated smaller currents than the wild type. Isoproterenol significantly prolonged APDs of LQT1 cardiomyocytes, while shortening those of healthy ones. A mathematical model for I_{Ks}-reduced human ventricular myocytes reproduced APD prolongation and generation of early afterdepolarizations (EADs) under β-adrenergic stimulation.

Conclusions: QT prolongation of the LQT1 patient with the mutation M437V of KCNQ1 was caused by I_{Ks} reduction, which may render the patient vulnerable to generation of EADs and arrhythmias.

Abbreviations: AP(D), action potential (duration); EAD, early afterdepolarization; EB, embryoid body; ESC, embryonic stem cell; HP, holding potential; I_{CaL}, L-type Ca^{2+} channel current; I_{Kr}, rapidly-activating delayed-rectifier K^+ channel current; I_{Ks}, slowly-activating delayed-rectifier K^+ channel current; I_{K1}, inward-rectifier K^+ channel current; I_{Na}, sodium channel current; iPSC, induced pluripotent stem cell; LQTS, long QT syndrome; TdP, Torsade de points.

* Corresponding author. Tel.: +81 76 286 4443; fax: +81 76 286 8010.
E-mail address: yasu@kanazawa-med.ac.jp (Y. Kurata).

Peer review under responsibility of the Japanese Society for Regenerative Medicine.

http://dx.doi.org/10.1016/j.reth.2015.12.001

1. Introduction

Long QT syndrome (LQTS) is characterized by prolonged QT intervals in ECG. It causes a specific form of tachycardia, Torsade de Pointes (TdP), which is driven by triggered activity through early afterdepolarization (EAD) and can cause sudden cardiac death [1–3]. LQTSs are classified into congenital and acquired ones [4]. Previous reports described at least 15 different forms of congenital LQTSs, 45% of which are caused by mutations in *KCNQ1* (*KvLQT1* or *Kv*7.1) and classified as LQTS type 1 (LQT1) [4–7]. *KCNQ1* encodes the alpha subunit of the channel generating slowly-activating delayed-rectifier K^+ currents (I_{Ks}) that are responsible for the repolarization of ventricular myocytes [2]. Mutations of KCNQ1 can cause (1) a reduction of KvLQT1 channel density on the plasma membrane due to trafficking defect and/or (2) impaired conductance of channels expressed in the plasma membrane. Heterologous expression systems and genetic animal models have been utilized to study the impacts of each mutation on protein trafficking and channel functions. However, they have several disadvantages such as artificial effects caused by overexpression of ion channels and inabilities to evaluate contributions of mutant channels to the action potential (AP) configuration in human cardiomyocytes [8,9]. Induced pluripotent stem cells (iPSCs) offer a unique opportunity to study the pathogenesis of a disease and screen appropriate therapeutic drugs [10]. Many studies have already shown that cellular phenotypes of inherited disorders are recapitulated by disease-specific iPSCs *in vitro*, and LQTSs are not exceptions [10,11].

We found a novel mutation, M437V, of KCNQ1 in a LQT1 patient. iPSCs were established from his T lymphocytes and differentiated into cardiomyocytes for analyzing their electrophysiological properties. The experimental results indicated an impaired activity of the mutant KvLQT1 channels to cause prolongation of AP durations (APDs); β-adrenergic stimulation (β-AS) augmented APD prolongation, while not inducing EADs. Computer simulations using a mathematical model of human ventricular myocytes suggested that EADs and arrhythmic behaviors could emerge in the mid-myocardial (M) cell layer of the ventricle when additional conditions to further prolong APDs occur.

2. Materials and methods

2.1. Patient consent

All subjects provided informed consent for genetic tests associated with LQTS. This study was approved by the Ethics Committee of Tottori University. It also conforms with the principles outlined in the Declaration of Helsinki for use of human tissue or subjects.

2.2. Establishment of T cell-derived iPSCs (TiPSCs) and culturing human embryonic stem cells (ESCs)

iPSCs were established as described previously [12]. Mononuclear cells were separated from the patient's blood by Ficoll–Paque PREMIUM (GE Healthcare). They were plated at 3.0×10^4 cells/cm^2 in 6-well plates coated with anti-human CD3 antibody (BD Pharmingen). They were incubated at 37.0 °C, with 3.0% CO_2 conditions. Cells were infected with Sendai virus carrying Yamanaka factors (DINAVEC); transfectants were plated at 5.0×10^5 in dish (MEF feeder) in the maintenance medium described previously [13,14], and cultured for 4 weeks. ESC-like colonies were transferred to 24-well plates on mouse embryonic fibroblast feeders. TiPSCs and human ESCs were cultured following the method of culturing human ESCs described by Suemori et al. [13].

2.3. Differentiation of TiPSCs and ESCs into cardiomyocytes

TiPSCs and human ESCs were differentiated into cardiomyocytes according to the protocol described by Yamauchi et al. [14]. In the process of iPSC induction from LQT1 patient T cells, 4 iPSC lines with typical stem cell morphology were selected and subjected to cardiac differentiation. We finally chose 2 lines (#b and #e) as patient-derived iPSC lines because they showed better cardiac differentiation. Both the cell line #b and #e showed very similar LQT1 phenotypes; the line #e was used as a representative. The same strategy was also applied for selection of healthy subject-derived iPSC lines, and the line #3 was used for analyses in this study.

2.4. Immunostaining

The primary antibodies for OCT4, SOX2, NANOG, TRA-1-60, TRA1-81, SSEA4 and tropomyosin used were Stem Light Pluripotency Antibody Kit (Cell Signaling Technology Danvers Massachusetts, USA) and MONOCLONAL ANTI-TROPOMIOSIN (Sigma–Aldrich, St Louis, MO, USA). To detect OCT4, SOX2, NANOG, TRA-1-60, TRA-1-81, SSEA4 and tropomyosin, fixed cells were stained with indicated monoclonal antibodies. Alexa Flulor 488-labeled or 546-labeled IgG (Molecular Probes Invitrogen, Carlsbad, CA) was used as the secondary antibody.

2.5. RT-PCR assay

Total RNAs were isolated using an RNeasy Micro Kit (QIAGEN, Tokyo, Japan). cDNAs were synthesized using PrimeScript® RT reagent Kit with gDNA Eraser Perfect Real Time (TaKaRa BIO, Otsu, Japan). RT-PCR was performed using EmeraldAmp® MAXPCR Master Mix (TaKaRa). Primer sequences are listed in the Supplemental Table 1.

2.6. Karyotype analysis

Karyotypes of iPSCs derived from the patient and healthy subject were determined using the standard Q-banding chromosome analysis.

2.7. Genomic sequencing

Genomic DNA was isolated from blood samples and TiPSCs derived from the patient and healthy subject. The KCNQ1 gene fragment was amplified by PCR and subjected to sequencing.

2.8. Plasmid construction and transfection

cDNAs encoding KCNQ1 were cloned in the plasmid pcDNA3.1 to create pcDNA3.1/KCNQ1. The mutation was introduced by site-directed mutagenesis. cDNAs encoding wild-type (WT) or M437V mutant KCNQ1 were ligated into the multiple cloning sites at pIRES-EGFP (Clontech, Mountain View, CA, USA) to create pIRES2-EGFP/WT KCNQ1 and pIRES2–EGFP/M437V KCNQ1. cDNAs encoding KCNE1 were also cloned in the pcDNA3.1. Both HEK293 and COS7 cells were cultured and co-transfected with pAcDsRed-Mem (membrane marker) and either pIRES2-EGFP/WT KCNQ1 or pIRES2–EGFP/M437V KCNQ1 together with pcDNA3.1/KCNE1 using lipofectamine (Invitrongen, Carlsbad, CA, USA). Cells were collected at 48 h after transfection and were subjected to assays.

2.9. Electrophysiological recordings

APs and ion channel currents were measured in the beating cells enzymatically isolated from embryoid bodies (EBs) under current clamp mode and voltage clamp mode, respectively, using the whole-cell patch-clamp technique. In the present study, we selectively collected ventricular type cells based on the morphological and electrophysiological criteria reported previously, i.e., elongated cells with an oval nucleus, well organized tension-oriented myofibrils spanning the long axis, relatively long AP plateau phase, and negative maximum diastolic potentials [15]. The external solution used to measure APs and ionic currents in iPSC-derived cardiomyocytes was the differentiation-inducing culture medium [13,14]. COS7 cells co-expressing KCNQ1 and KCNE1, visualized by GFP fluorescence, were also subjected to the whole-cell patch clamp to measure the WT KCNQ1/KCNE1 or M437V KCNQ1/KCNE1-medicated current corresponding to I_{Ks} in the culture medium.

The glass pipettes had a resistance of 6–8 MΩ after filling with the internal pipette solution containing (in mM) 100 K-aspartate, 20 KCl, 1 $CaCl_2$, 5 Mg-ATP, 5 ethylene glycol bis(2-aminoethylether)-N,N,N′,N'-tetraacetic acid (EGTA), 5 HEPES, and 5 creatine phosphate (pH 7.2 with KOH). Currents were recorded using an Axopatch-200B amplifier (Axon Instrument, USA) and directly stored in a personal computer (NEC Mate, Japan) at 10 kHz. The capacity-corrected data were digitally filtered at 2 kHz and analyzed with the pCLAMP9 software.

Outward membrane currents of I_{Ks} and KCNQ1/KCNE1-medicated currents were elicited every 6 s by 4000-ms depolarizing test pulses ranging from −40 to +60 mV (in 10 mV increments), which were followed by 1500-ms repolarization to −40 mV for recording tail currents. A holding potential (HP) was −60 mV. I_{Ks} in iPSC- and ESC-derived cardiomyocytes was measured as a chromanol 293B-sensitive current, separated by applying chromanol 293B at 50 μM.

Voltage dependence of I_{Ks} activation determined by measurements of the tail current amplitude during repolarizing pulses was fitted by a Boltzmann equation as a function of membrane potentials (V_m):

$$I_{Ks,tail} = 1/\{1 + \exp[-(V_m - V_h)/s]\}, \quad (1)$$

where $I_{Ks,tail}$ represents the current amplitude normalized to the maximum attainable current. V_h and s denote the half-maximum voltage and slope factor, respectively.

Na^+ channel current (I_{Na}) and Ca^{2+} channel current (I_{Ca}) were elicited at 0.2 Hz by 100-ms depolarization to −80 ~ +60 mV (in 10 mV increments) from a HP of −90 and −50 mV, respectively. Rapidly-activating delayed-rectifier K^+ channel current (I_{Kr}) was evoked by 200-ms test pulses ranging from −40 to +50 mV (in 10 mV increments) from a HP of −80 mV; tail currents of I_{Kr} were measured by clamping back to −50 mV. In addition, the inward-rectifier K^+ channel current (I_{K1}) was recorded using a ramp pulse protocol with a functional generator (FG-122, NF Corporation). The ramp pulses ranging from −120 to 0 mV were applied at 1.5 V/s every 3 s. For cells with automaticity, the beating rate was measured by a time lapse imaging system (LCV110, Olympus). All experiments were carried out at 37 °C.

2.10. Statistical analysis

All values are presented as the mean ± S.E.M. For statistical analysis, repeated-measures analysis of variance (two-way ANOVA) was used, with $p < 0.05$ considered statistically significant. Statistical analyses and nonlinear curve fittings were performed with Origin 8.5 (OriginLab, MA, USA).

2.11. Computer simulations of APs of human cardiac myocytes

We simulated prolongation of APDs and EAD generations in LQT1 cardiomyocytes using a mathematical model of human ventricular myocytes developed by Kurata et al. [16]. A M cell version of the model cell was developed on the basis of the transmural heterogeneity in densities of ion channels and transporters as summarized by O'Hara et al. [17]. We employed the M cell version, because it has larger I_{CaL}, as well as smaller I_{Kr} and I_{Ks}, thus being much more vulnerable to EAD formation than the endocardial and epicardial versions [17]; it was most advantageous to recapitulating EADs under the conditions of β-AS and arrhythmogenicity of LQT1. APs were elicited by 1-ms stimuli of 60 pA/pF at 1 Hz. For simulating the conditions of β-AS as a major trigger of EADs and TdP in LQT1, parameters describing the maximum conductance of ion channels and density of transporters were modified on the basis of previous reports [18,19] as follows: (1) the maximum I_{CaL} conductance (g_{CaL}) increased to 200–350% of the control; (2) the maximum I_{Ks} conductance (g_{Ks}) increased twice with the voltage dependence of activation kinetics negatively shifted by 8 mV; (3) Na^+-K^+ pump current density increased by 20%; and (4) sarcoplasmic reticulum Ca^{2+} pumping rate increased by 41%.

3. Results

3.1. Clinical characteristics of the patient

An 18-year-old man was diagnosed as LQTS by standard 12-lead ECG, which showed a prolonged heart rate-corrected QT interval (QTc) of 462 ms as compared with the QTc (381 ms) of one healthy volunteer (Fig. 1A). The ECG suggested the diagnosis of LQT1. His father and sister, who also have the same M437V mutation, showed similar QT interval abnormality (Fig. 1B). There were no abnormal findings in chest X-ray, ultrasonic cardiogram or treadmill exercise test. Direct sequencing of *KCNQ1* alleles identified a mutation, A1309G, in one allele (Fig. 1C), which causes the M437V mutation in KCNQ1 (Fig. 1D). No mutation was found in the major LQTS-related genes KCNH2, SCN5A, KCNE1 or KCNE2.

3.2. Generation of iPSCs

To generate iPSCs, we used T lymphocytes from the LQT1 patient and healthy volunteer; they were reprogrammed by Sendai virus-mediated gene transfer of OCT3/4, SOX2, KLF4, and c-MYC. Several clones were generated, expanded, and stored. As exemplified in the supplemental Fig. S1A, all iPSC lines showed typical iPSC morphology. Qualitative RT-PCR confirmed that all lines expressed pluripotency markers such as OCT3/4, SOX2, KLF4, c-MYC and NANOG, as well as silenced exogenous genes (Fig. S1B). Immunohistochemistry also confirmed expressions of the pluripotency markers OCT3/4, SOX2, SSEA4, TRA-1-60, TRA-1-81 and NANOG (Fig. S1C). Chromosome analysis showed no abnormality of their karyotypes (supplemental Fig. S2). We selected two clones of iPSCs from the LQT1 patient and two clones of iPSCs from the healthy subject for further characterizations after cardiac differentiation.

3.3. Differentiation of iPSCs and human ESCs into cardiomyocytes

iPSCs and human ESCs were differentiated into cardiomyocytes in EBs. Cells in EBs started spontaneous beating in 1 week after formation of EBs. There was no significant difference in characteristics of iPSC-derived cardiomyocytes between the LQT1

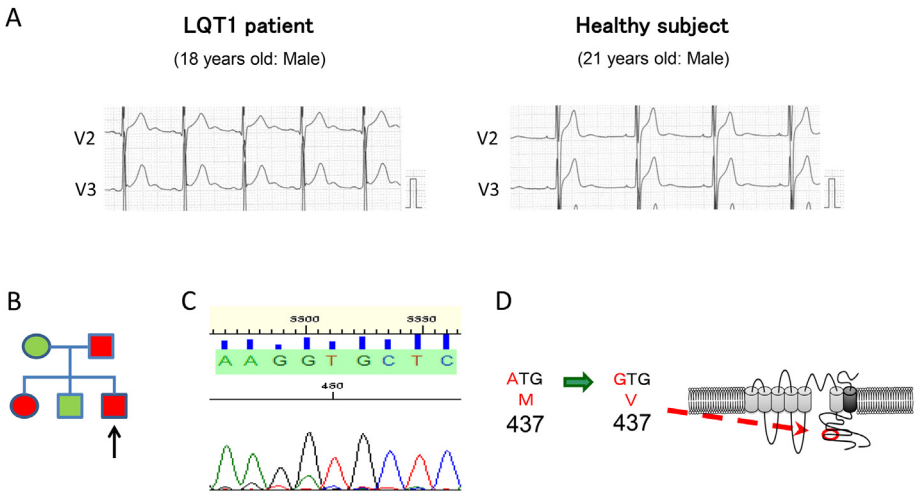

Fig. 1. Characterization of a LQT1 patient with the M437V mutant KCNQ1. (A) ECGs of the LQT1 patient and a healthy subject as a control, which show the QTc values of 462 and 381 ms, respectively. (B) The family pedigree of the proband with LQT1. The arrow indicates the patient. The members with the M437V mutation and QT prolongation are shown in red. (C) A novel KCNQ1 mutation of A1309G (M437V) in the LQT1 patient. The sequence analysis of genomic KCNQ1 obtained from blood of the patient and healthy subject revealed a heterozygote missense mutation (A→G) at the position 1309 of the KCNQ1 coding region (A1309G). (D) A schematic representation of the mutant KCNQ1 protein, indicating the substitution of the uncharged valine for the positively charged methionine at the position 437 of the cytoplasmic C-terminal domain (M437V).

patient and healthy subject: Both EBs developed from healthy subject-derived and LQT1 patient-derived iPSCs showed similar mRNA levels of TnT, MYH6, MYL2, MYL7, KCNQ1 and KCNE1 as evaluated by RT-PCR (Fig. 2A). Enzymatically dissociated cardiomyocytes were positively stained with anti-tropomyosin antibody (Fig. 2B).

3.4. Comparison of electrophysiological properties of cardiomyocytes derived from healthy subject iPSCs, LQT1 patient iPSCs and human ESCs

Fig. 3A shows the representative traces of ventricular type APs recorded from a healthy subject and an LQT1 patient iPSC-derived

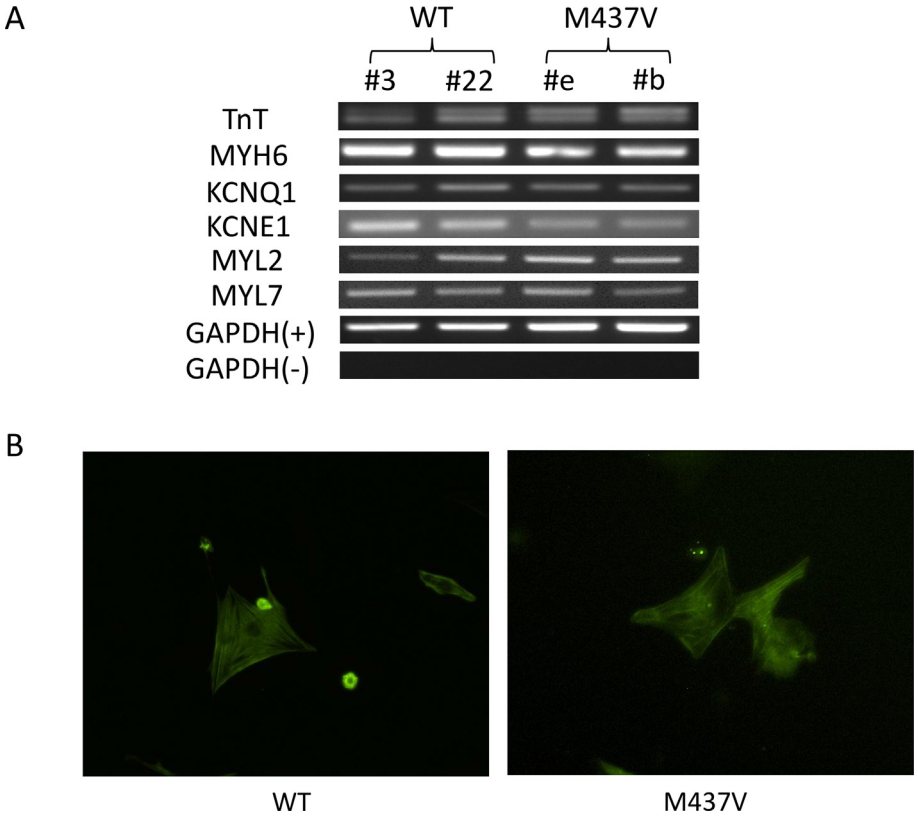

Fig. 2. Cardiac differentiation of iPSCs obtained from the LQT1 patient (M437V) and healthy subject (WT). (A) Representative mRNA expressions of cardiac markers in cardiomyocytes differentiated from iPSCs of the patient and healthy subject. (B) Representative immunofluorescence analysis of tropomyosin expression in cardiomyocytes differentiated from the patient and healthy subject iPSCs.

cardiomyocyte as well as a human ESC-derived cardiomyocyte. APDs were longer in the LQT1 iPSC-derived cardiomyocyte than in the healthy iPSC- and human ESC-derived one. There were no differences in diastolic membrane potentials among them. Fig. 3B shows summary data of APDs at 50% repolarization (APD_{50}) and 90% repolarization (APD_{90}) obtained from 15 healthy and 15 LQT1 iPSC-derived cardiomyocytes as well as 15 human ESC-derived ones. APDs were significantly longer in LQT1 iPSCs-derived cardiomyocytes.

Fig. 4A shows representative outward membrane currents recorded from a healthy and an LQT1 iPSC-derived cardiomyocyte as well as a human ESC-derived one. These currents were almost completely blocked by 50 μM chromanol 293B (data not shown), indicating that they correspond to I_{Ks}. The amplitude of I_{Ks} measured as a chromanol 293B-sensitive current was smaller in LQT1 iPSC-derived cardiomyocytes than in the others; time courses of voltage-dependent activation and deactivation were comparable. Voltage dependences of I_{Ks} activation measured at the end of depolarizing test pulses are summarized in Fig. 4B. Fig. 4C shows voltage dependences of the tail current amplitude measured as the maximum at the beginning of each repolarizing pulse and normalized to the maximal attainable current at the most depolarized potential (+60 mV) for the three types of cardiomyocytes. The sigmoidal curves are the fits by the Boltzmann equation (Eq. (1)). They overlapped with each other with similar time constants of activation and deactivation, indicating the normal gating kinetics of I_{Ks} channels in the LQT1 cardiomyocyte. I_{Ks} amplitudes at +60 mV were 11.33 ± 1.76 pA/pF for the healthy iPSC-derived cardiomyocyte and 4.99 ± 0.54 pA/pF for the M437V iPSC-derived one; thus, the maximum conductance of the mutant channel was estimated to be 44% of the normal one. As shown in the supplemental Fig. S3, I_{Na}, I_{Ca}, I_{Kr} or I_{K1} showed no significant differences in amplitude or kinetics among the three types of cardiomyocytes. Taken together, the LQT1 iPSC-derived cardiomyocyte had specific reductions in conductance of KvLQT1-mediated I_{Ks}.

3.5. Characterization of heterologously-expressed mutant KCNQ1 proteins and channels

Some mutations of KCNQ1 impair protein trafficking, resulting in reduced expression of KCNQ1 on the plasma membrane. To examine the intracellular trafficking of M437V mutant KCNQ1 proteins, they were expressed in HEK293 cells. As illustrated in Fig. 5, both signals of the WT and mutant KCNQ1-GFP similarly merged with the signals of membrane markers, indicating their normal trafficking to the plasma membrane. We also measured KCNQ1-mediated currents in COS7 cells expressing the WT or mutant KCNQ1-GFP. Fig. 6A shows representative traces of KCNQ1-mediated currents in COS7 cells transfected with either the WT or mutant KCNQ1 plasmid. As shown in Fig. 6B summarizing the voltage-dependent activation of KCNQ1-mediated currents, the amplitude of the mutant KCNQ1-mediated currents was significantly smaller than that of the WT currents.

3.6. Effects of isoproterenol on AP properties of LQT1 iPSCs-derived cardiomyocytes

Fig. 7 shows the effects of isoproterenol on AP waveforms of cardiomyocytes derived from healthy and LQT1 iPSCs. Isoproterenol (100 nM) remarkably prolonged APDs of LQT1 iPSC-derived cardiomyocytes, while shortening APDs of healthy iPSC-derived ones.

3.7. Computer simulations of APD prolongation and EAD generation in LQT1 cardiomyocytes

Fig. 8A shows simulated APs of the normal and LQT1 model cardiomyocytes (M cells) under the basal (control) condition and conditions of β-AS with g_{CaL} increased by 100, 200 or 250%. LQT1 model cells were developed by reducing g_{Ks} to 44% and 24% of the control, according to the current density data for the M437V mutation (Fig. 4) and the previous report for the A590W mutation [20], respectively. The LQT1 model cells showed longer APDs

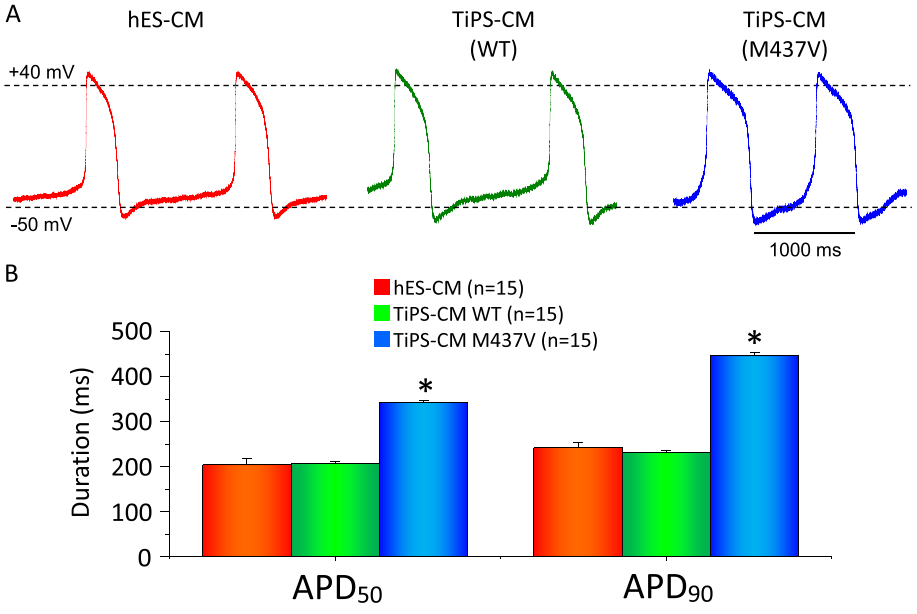

Fig. 3. Action potential (AP) properties of iPSC-derived cardiomyocytes (TiPS-CM) obtained from the LQT1 patient (M437V) and healthy subject (WT) as well as human ESC-derived ones (hES-CM). (A) Representative spontaneous APs recorded from differentiated cardiomyocytes. (B) Summary data of the AP duration at 50% repolrarization (APD_{50}) and 90% repolrarization (APD_{90}) from the 3 types of cardiomyocytes (n = 15 each).

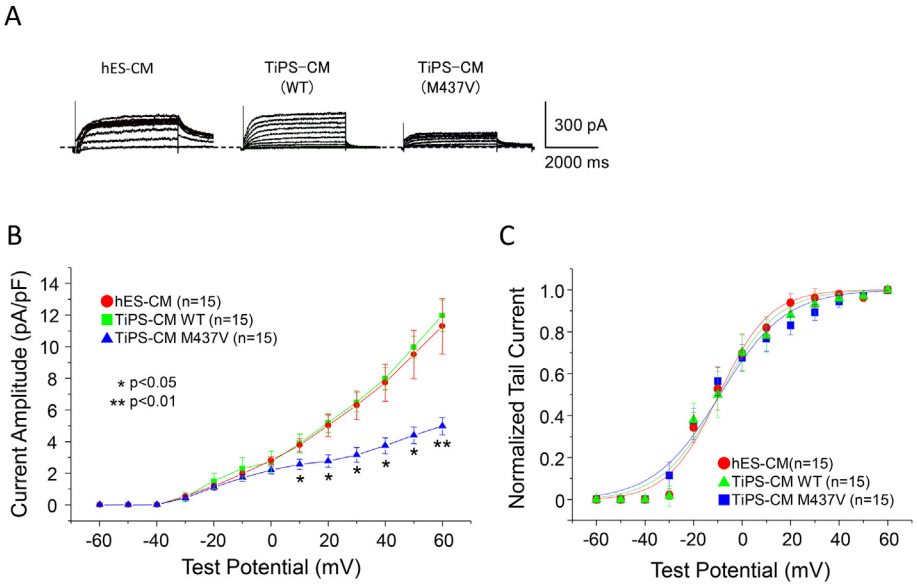

Fig. 4. Kinetic properties of I_{Ks} in iPSC-derived cardiomyocytes (TiPS-CM) obtained from the LQT1 patient (M437V) and healthy subject (WT) as well as human ESC-derived ones (hES-CM). (A) Representative original traces of chromanol 293B-sensitive currents corresponding to I_{Ks}, which were elicited by the depolarizing test pulses ranging from −40 to +60 mV in the presence of 50 μM chromanol 293B. (B) Voltage dependence of I_{Ks} activation. The amplitudes of currents at the end of depolarizing test pulses were determined and plotted against the test potentials for the 3 types of cardiomyocytes (n = 15 each). (C) Voltage-dependent activation of the tail currents. The maximum current amplitudes determined at the beginning of repolarizing pulses were normalized to the maximum attainable current and plotted against depolarizing test potentials for the 3 types of cardiomyocytes (n = 15 each). The curves are the fits with the Boltzmann equation (Eq. (1)); the half-maximum potentials estimated for the patient (M437V) iPSC-, healthy (WT) iPSC- and human ESC-derived cardiomyocytes were −9.08, −9.17 and −9.57 mV, respectively.

under the basal condition (429 ms in normal vs. 486 ms in M437V and 525 ms in A590W) and EAD generations under β-AS with g_{CaL} increased by 250% in M437V and 100% (or more) in A590W, whereas the normal cell never exhibited EADs. Susceptibility of the normal and LQT1 cardiomyocytes to EAD generation during β-AS is compared in Fig. 8B, where critical values of g_{CaL} for EAD generation (and EAD termination leading to repolarization failure) are plotted as a function of g_{Ks}. EAD generation via g_{CaL} increases during β-AS can be avoided by concomitant g_{Ks} increases in the normal cell, but not in the LQT1 cells. The g_{CaL} increase required for EAD formation is larger in M437V (250%) than in A590W (90%). As shown in the supplemental Fig. S4 for M437V, however, concomitant reductions in the maximum I_{Kr} conductance (g_{Kr}) dramatically lower the critical g_{CaL} value to cause EADs. Susceptibility of the cardiomyocytes to EAD generation was also tested for inhibition of I_{Kr} alone without β-AS (supplemental Fig. S5). The distances from the control condition to the critical point to cause EADs during increases in g_{CaL} or decreases in g_{Kr}, i.e., the degrees of g_{CaL} increases or g_{Kr} decreases required for EAD formation are much smaller in the LQT1 model cells than in the normal one. These results indicate that susceptibility to EAD generation during β-AS (enhancement of I_{CaL}) and/or inhibition of I_{Kr} was much higher in the LQT1 cardiomyocytes than in the normal one.

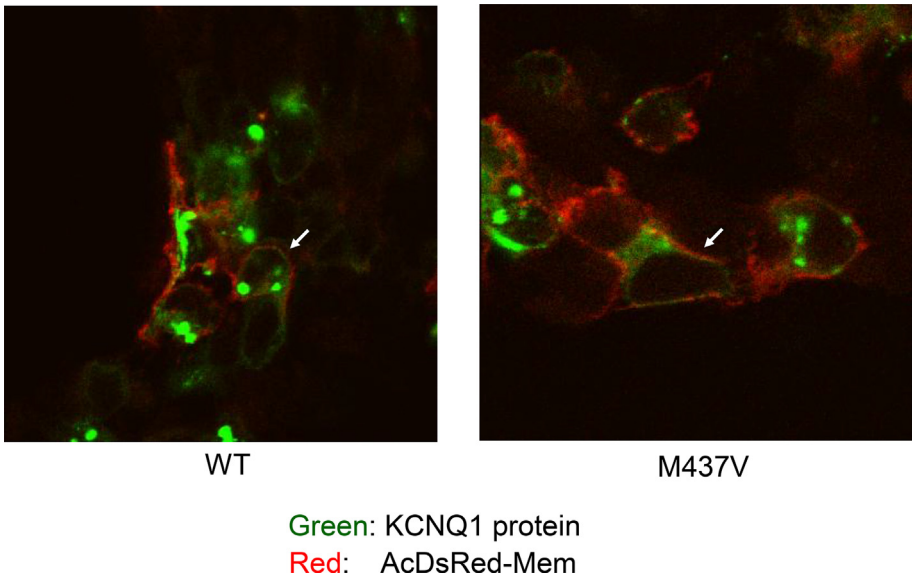

Fig. 5. Expressions of the wild-type (WT) and M437V mutant KCNQ1-GFP in HEK293 cells co-expressing WT KCNE1. Shown are representative immunofluorescence images of WT or M437V KCNQ1-GFP and a membrane marker, AcDsRed-Mem.

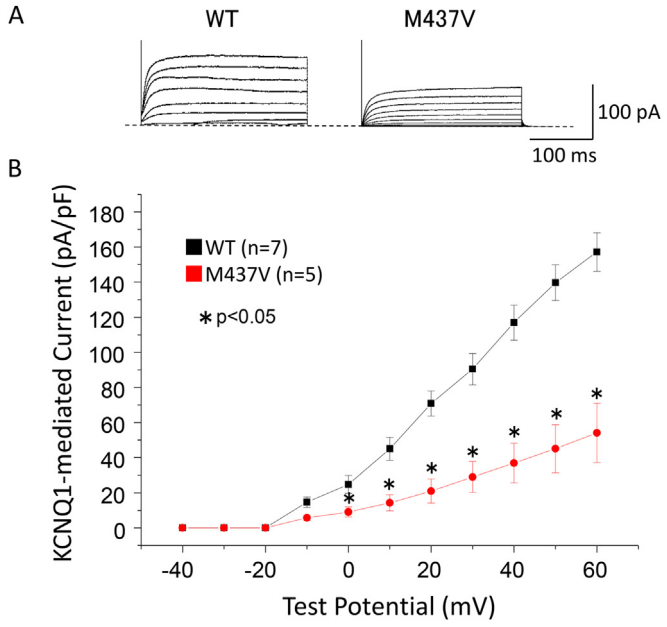

Fig. 6. Membrane currents mediated by the WT and M437V mutant KCNQ1 expressed in COS7 cells. (A) Representative traces of WT and M437V KCNQ1-mediated currents in COS7 cells co-expressing WT KCNE1. (B) Voltage-dependent activation of WT and M437V KCNQ1-mediated currents. The amplitudes of currents at the end of depolarizing test pulses were determined and plotted against test potentials for COS7 cells expressing WT KCNQ1-GFP (n = 7) or M437V KCNQ1-GFP (n = 5) together with WT KCNE1.

4. Discussion

In the present study, we developed iPSCs and iPSC-derived cardiomyocytes from T cells of a case with familial LQT1 harboring the missense mutation M437V of KCNQ1 in order to determine electrophysiological properties of cardiomyocytes with the mutant KCNQ1. Infection by Sendai virus harboring Yamanaka 4 factors generated iPSCs without any genome injury [12]. Obtained iPSCs expressed mRNA of the endogenous pluripotent markers without residual exogenous Sendai virus vectors (Fig. S1B). Pluripotency has been confirmed by protein expressions of the pluripotent markers (Fig. S1C). iPSCs from the patient as well as a healthy subject differentiated into cardiomyocytes in EBs (Fig. 2).

KvLQT1 channels coded by *KCNQ1* confer I_{Ks}, which is responsible for repolarization of cardiomyocytes. Mutations of *KCNQ1* to cause LQT1 can reduce I_{Ks} and prolong APDs by two mechanisms: 1) impaired trafficking of KCNQ1 proteins to the plasma membrane [7,10], and 2) impaired functions of channel proteins expressed in the membrane [21]. Compared with the healthy iPSC- and human ESC-derived cardiomyocytes, the cardiomyocytes derived from the LQT1 patient iPSCs showed a significant reduction in I_{Ks} and prolonged APDs without differences in I_{Na}, I_{Ca}, I_{Kr} or I_{K1}. There was no difference in traffic between the mutant and WT KCNQ1 proteins when expressed in HEK293 cells. KCNQ1-mediated currents were significantly smaller in COS7 cells transfected with the mutant KCNQ1 than in those transfected with the WT. Taken together, the mutation M437V reduced I_{Ks} and prolonged APDs via the second mechanism. There was no significant difference in voltage-dependent kinetics of I_{Ks} between the LQT1 and healthy cells, suggesting that the single channel conductance is reduced in the mutant channel. Single channel recordings are necessary to further characterize the electrophysiological properties of the mutant channel.

A KCNQ1 subunit has six transmembrane domains with intracellular N- and C-termini [7]. I_{Ks} channels are constructed by tetramers of KCNQ1 subunits with or without a KCNE1 subunit, a single transmembrane domain peptide [22–26]. It is predicted that the C-terminal domain of KCNQ1 contains four α-helices (helices A, B, C and D), which play an important role in protein folding, tetoramerization and KCNE1 binding. Helices A and B harbor binding sites for calmodulin that is responsible for proper folding of the C-terminal region [24,27,28], whereas helices C and D play an

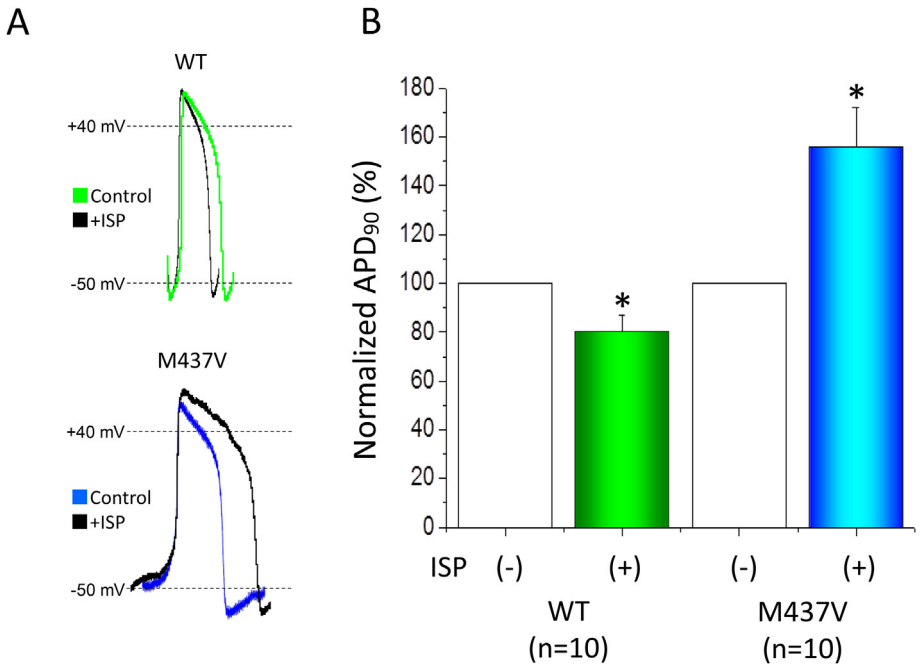

Fig. 7. Effects of isoproterenol (ISP) on APs of cardiomyocytes derived from healthy (WT) and LQT1 (M437V) iPSCs. (A) Representative APs of iPSC-derived cardiomyocytes in the absence (green/blue) and presence (black) of 100 nM ISP. (B) Summary data of changes in APDs by 100 nM ISP (n = 10 each). APD_{90} values (averages from three APs) were determined before and after a 5 min application of ISP; the value with ISP (ISP(+)) was normalized to the control value (ISP(−)). *p < 0.05 vs. each control (ISP(−)), paired t-test.

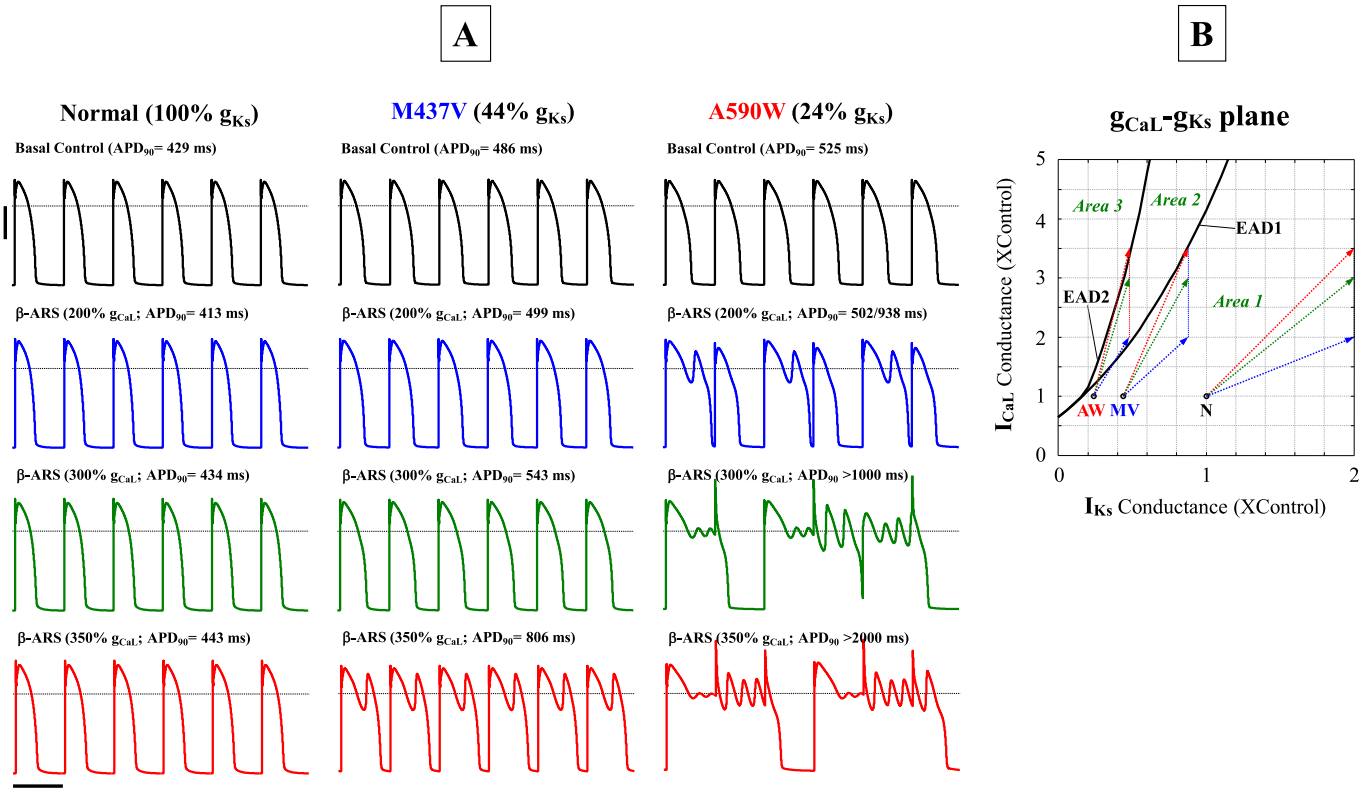

Fig. 8. I_{CaL}-dependent electric behaviors of the normal and LQT1 ventricular myocyte (M cell) models under β-AS. The LQT1 model cells were developed by reducing g_{Ks} to 44% (M437V) and 24% (A590W) of the control. For simulating the conditions of β-AS, parameters other than the maximum conductance of I_{CaL} (g_{CaL}) and I_{Ks} (g_{Ks}) were modified on the basis of the previous reports as stated in the Methods section. (A) Simulated APs of the model cells under the basal condition and conditions of β-AS with g_{CaL} increased to 200, 300 or 350% of the control value. Model cells were paced at 1 Hz with 1-ms stimuli of 60 pA/pF for 30 min; the AP responses evoked by the last 6 stimuli are shown. The horizontal and vertical solid lines indicate 1 s and 40 mV, with the dashed lines denoting the 0 mV level. (B) Critical values of g_{CaL} for the initiation (EAD1) and termination (EAD2) of EADs plotted as a function of g_{Ks}. The point for EAD termination (EAD2) was determined as the point at which repolarization failure (i.e., low-voltage oscillations or arrest at depolarized potentials) occurred. The maximum conductance of each current is indicated as a ratio to the control value. The model cell was paced at 1 Hz with 1-ms stimuli of 60 pA/pF for 1–2 min at each parameter set. The critical points were determined during g_{CaL} increases under β-AS at various g_{Ks} values. The parametric planes were divided into 3 areas by the loci of the critical points: (1) normal APs (Area 1), (2) APs with EADs (Area 2), and (3) repolarization failure (Area 3). The points of the control conditions for cardiomyocytes with the normal, M437V mutant and A590W mutant I_{Ks} are labeled as "N", "MV" and "AW", respectively, with the arrows indicating the β-AS-induced parameter shifts from the control condition to the points (parameter sets) at which AP behaviors were tested as shown in Panel A.

important role in trafficking and tertramerization [25,26]. Previous reports indicated that mutations of KCNQ1 located in the helices A and B led to the impaired stability of KCNQ1, resulting in the impaired membrane trafficking [23,26]. In the present study, however, the M437V mutation located in the flanking region of helices A and B led to a reduction in channel currents with normal trafficking. Thus, this is the first report indicating that a mutation in the region of helices A and B can influence the conductance of KCNQ1-mediated channel currents without impaired traffic to the plasma membrane.

It remains unknown whether the impaired functions of KvLQT1 channels could underlie the prolongation of ventricular APD and QTc in the present case. As demonstrated by the computer simulation using the human ventricular myocyte model, the 56% reduction of the KvLQT1 channel current I_{Ks} as observed in this mutation (Fig. 4) yielded the 13.4% prolongation of human ventricular (M cell) APDs during 1 Hz pacing. This result suggests that the reduction of I_{Ks} observed in the present LQT1 iPSC-derived cardiomyocytes could underlie the prolongation of ventricular APD and QTc.

It is also an issue whether this impaired I_{Ks} channel activity could lead to arrhythmogenicity in the present case, since the present case did not have a medical history of TdP or syncope. The previous studies reported that isoproterenol, as well as the I_{Kr} inhibitor E4031, induced triggered activities following EADs in the cardiomyocytes derived from iPSCs of LQT1 patients, which have been prevented by pretreatment with β-blockers [7,10]. In our experiments using iPSC-derived cardiomyocytes with the M437V mutation, administration of isoproterenol and/or E4031 prolonged APDs but did not induce EADs or arrhythmic behaviors, which might support less arrhythmogenicity in the present case. Based on our simulations (Fig. 8, S4 and S5), however, EADs may occur in this LQT1 patient when a larger increase in I_{CaL} is induced by stronger β-AS (e.g., via catecholamine administration) and/or when I_{Kr} is inhibited (e.g., by application of calss III antiarrhythmic agents). Greater enhancement of I_{CaL} and/or greater inhibition of I_{Kr} were required for EAD formation in M437V (44% g_{Ks}) than in A590W (24% g_{Ks}), which may account for the lack of a medical history in the present case. Nonetheless, the impaired activity of the M437V mutant I_{Ks} as estimated from iPSCs-derived cardiomyocytes may lead to generation of EADs and resultant TdP during β-AS in combination with concomitant inhibitions of I_{Kr} or delay in β-AS-induced I_{Ks} increases, although it could not induce EADs or TdP under basal conditions or relatively weak β-AS. These findings might be useful in managing the risk of this case and also explain the less arrhythmogenicity (lack of clinical events) in the present case.

Priori et al. stratified clinical risk according to the genotype, in conjunction with other clinical variables such as sex and length of the QT interval [29]. The QTc was an independent predictor of risk

among patients with a mutation at the LQT1 locus, since cardiac event-free survival was greater in both male and female patients with QTc of <500 ms than in those with QTc of >500 ms. The present case showed the QTc less than 500 ms (462 ms) without any family history of sudden cardiac death, predicting the less chance of cardiac events. As suggested by the simulation study (Fig. 8, S4 and S5), however, the LQT1 patient with the M437V mutation would be much more vulnerable to the generation of EADs and TdP than healthy subjects, especially under pathophysiological and/or therapeutic conditions, such as hypokalemia and administration of catecholamine and/or class III antiarrhythmic agents, leading to further increases in QTc [30].

It is obvious that the present study includes a certain limitation. Comparison of iPSCs generated from patients with those from healthy control is not reasonable, because the influences of gene polymorphisms other than the focused mutation could not be ruled out. It is most reasonable to make isogenic control using genome editing technologies such as CRISPR/Cas9 or TALEN for elucidating pure effects of the M437V mutation; however, we did not create the isogenic control in this study. To compensate for this limitation, we evaluated electrophysiological properties of the human ESC-derived cardiomyocyte as another control, which is frequently used as a control for comparisons to iPSC-derived ones [31]. The electrophysiological properties of human ESC-derived cardiomyocytes were comparable to those of healthy iPSC-derived ones.

5. Conclusion

This study has demonstrated for the first time that a mutation in the KCNQ1 region of helices A and B can reduce the conductance of KCNQ1-mediated I_{Ks} channel currents without trafficking defect. The reduced I_{Ks} of the M437V mutant channel could account for the prolongation of APD in iPSC-derived cardiomyocytes and QTc in ECG of the patient. The lack of a medical history in this case might be due to the relatively small reduction in current amplitude of the mutant channel; however, the patient would be much more vulnerable to the generation of EADs and TdP than healthy subjects under pathophysiological and/or therapeutic conditions. The present study indicates that a combination of electrophysiological study using LQT1 iPSC-derived cardiomyocytes and computer simulation study is useful not only for elucidating the mechanisms of arrhythmogenicity in LQTSs but also for evaluation of future risk for arrhythmias.

Acknowledgments

This study was supported by Grant in-Aid for Scientific Research from the Ministry of Education, Culture, Science, Sports and Technology of Japan (15K21170 and 25893134 to K.M., 25136720 and 26460303 to Y.K., 26501003 to Y.S. and 25670110 to I.H.), the Cooperative Research Program of Institute for Frontier Medical Sciences, Kyoto University, Japan (to Y.S.), and Grant for Collaborative Research from Kanazawa Medical University (C2015-3 to Y.K. and I.H.).

Appendix A. Supplementary data

Supplementary data related to this article can be found at http://dx.doi.org/10.1016/j.reth.2015.12.001.

References

[1] Priori SG, Bloise R, Crotti L. The long QT syndrome. Europace 2001;3:16–27.
[2] Moss AJ, Shimizu W, Wilde AAM, Towbin JA, Zareba W, Robinson JL, et al. Clinical aspects of type-1 long-QT syndrome by location, coding type, and biophysical function of mutations involving the KCNQ1 gene. Circulation 2007;115:2481–9.
[3] Roden DM. Long-QT syndrome. N Engl J Med 2008;358:169–76.
[4] Beitland S, Platou ES, Sunde K. Drug-induced long QT syndrome and fatal arrhythmias in the intensive care unit. Acta Anaesthesiol Scand 2014;58:266–72.
[5] Bhuiyan ZA, Al-Shahrani S, Al-Aama J, Wilde AAM, Momenah TS. Congenital long QT syndrome: an update and present perspective in Saudi Arabia Front. Front Pediatr 2013;1:39.
[6] Mizusawa Y, Horie M, Wilde AA. Genetic and clinical advances in congenital long QT syndrome. Circ J 2014;78:2827–33.
[7] Moretti A, Bellin M, Welling A, Jung CB, Lam JT, Bott-Flügel L, et al. Patient-specific induced pluripotent stem-cell models for Long-QT syndrome. N Engl J Med 2010;363:1397–409.
[8] Hofmann F, Lacinova L, Klugbauer N. Voltage-dependent calcium channels: from structure to function. Rev Physiol Biochem Pharmacol 1999;139:33–87.
[9] Ludwig A, Zong X, Jeglitsch M, Hofmann F, Biel M. A family of hyperpolarization-activated mammalian cation channels. Nature 1998;393:587–91.
[10] Egashira T, Yuasa S, Suzuki T, Aizawa Y, Yamakawa H, Matsuhashi T, et al. Disease characterization using LQTS-specific induced pluripotent stem cells. Cardiovasc Res 2012;95:419–29.
[11] Itzhaki I, Maizels L, Huber I, Zwi-Dantsis L, Caspi O, Winterstern A, et al. Modelling the long QT syndrome with induced pluripotent stem cells. Nature 2011;471:225–9.
[12] Seki T, Yuasa S, Oda M, Egashira T, Yae K, Kusumoto D, et al. Generation of induced pluripotent stem cells from human terminally differentiated circulating T cells. Cell Stem Cell 2010;7:11–4.
[13] Suemori H, Yasuchika K, Hasegawa K, Fujioka T, Tsuneyoshi N, Nakatsuji N. Efficient establishment of human embryonic stem cell lines and long-term maintenance with stable karyotype by enzymatic bulk passage. Biochem Biophys Res Commun 2006;345:926–32.
[14] Yamauchi K, Sumi T, Minami I, Otsuji TG, Kawase E, Nakatsuji N, et al. Cardiomyocytes develop from anterior primitive streak cells induced by β-catenin activation and the blockage of BMP signaling in hESCs. Genes Cells 2010;15:1216–27.
[15] Hescheler J, Fleischmann BK, Lentini S, Maltsev VA, Rohwedel J, Wobus AM, et al. Embryonic stem cells: a model to study structural and functional properties in cardiomyogenesis. Cardiovasc Res 1997;36:149–62.
[16] Kurata Y, Hisatome I, Matsuda H, Shibamoto T. Dynamical mechanisms of pacemaker generation in I_{K1}-downregulated human ventricular myocytes: insights from bifurcation analyses of a mathematical model. Biophys J 2005;89:2865–87.
[17] O'Hara T, Virág L, Varró A, Rudy Y. Simulation of the undiseased human cardiac ventricular action potential: model formulation and experimental validation. PLoS Comput Biol 2011;7:e1002061,. http://dx.doi.org/10.1371/journal.pcbi.1002061 [accessed January 15, 2015].
[18] Zeng J, Rudy Y. Early after depolarizations in cardiac myocytes: mechanism and rate dependence. Biophys J 1995;68:949–64.
[19] Kuzumoto M, Takeuchi A, Nakai H, Oka C, Noma A, Matsuoka S. Simulation analysis of intracellular Na^+ and Cl^- homeostasis during β1-adrenergic stimulation of cardiac myocyte. Prog Biophys Mol Biol 2008;96:171–86.
[20] Wiener R, Haitin Y, Shamgar L, Fernández-Alonso MC, Martos A, Chomsky-Hecht O, et al. The KCNQ1 (Kv7.1) COOH terminus, a multitiered scaffold for subunit assembly and protein interaction. J Biol Chem 2008;283:5815–30.
[21] Chen J, Zheng R, Melman YF, McDonald TV. Functional interactions between KCNE1 C-terminus and the KCNQ1 channel. PLoS One 2009;4:e5143. http://dx.doi.org/10.1371/journal.pone.0005143 [accessed January 15, 2015].
[22] Schwake M, Athanasiadu D, Beimgraben C, Blanz J, Beck C, Jentsch TJ, et al. Structural determinants of M-type KCNQ (Kv7) K+ channel assembly. J Neurosci 2006;26:3757–66.
[23] Shamgar L, Ma L, Schmitt N, Haitin Y, Peretz A, Wiener R, et al. Calmodulin is essential for cardiac I_{KS} channel gating and assembly: impaired function in long-QT mutations. Circ Res 2006;98:1055–63.
[24] Ghosh S, Nunziato DA, Pitt GS. KCNQ1 assembly and function is blocked by long-QT syndrome mutations that disrupt interaction with calmodulin. Circ Res 2006;98:1048–54.
[25] Howard RJ, Clark KA, Holton JM, Minor DL. Structural insight into KCNQ (Kv7) channel assembly and channelopathy. Neuron 2007;53:663–75.
[26] Wiener R, Haitin Y, Shamgar L, Fernandez-Alonso MC, Martos A, Chomsky-Hecht O, et al. The KCNQ1 (Kv7.1) COOH terminus, a multitiered scaffold for subunit assembly and protein interaction. J Biol Chem 2008;283:5815–30.
[27] Wen H, Levitan IB. Calmodulin is an auxiliary subunit of KCNQ2/3 potassium channels. J Neurosci 2002;22:7991–8001.
[28] Yus-Najera E, Santana-Castro I, Villarroel A. The identification and characterization of a noncontinuous calmodulin-binding site in noninactivating voltage-dependent KCNQ potassium channels. J Biol Chem 2002;277:28545–53.
[29] Priori SG, Schwartz PJ, Napolitano C, Bloise R, Ronchetti E, Grillo M, et al. Risk stratification in the long-QT syndrome. N Engl J Med 2003;348:1866–74.
[30] Imai M, Nakajima T, Kaneko Y, Niwamae N, Irie T, Ota M, et al. A novel KCNQ1 splicing mutation in patients with forme fruste LQT1 aggravated by hypokalemia. J Cardiol 2014;64:121–6.
[31] Bellin M, Casini S, Davis RP, D'Aniello C, Haas J, Ward-van Oostwaard D, et al. Isogenic human pluripotent stem cell pairs reveal the role of a KCNH2 mutation in long-QT syndrome. EMBO J 2013;32:3161–75.